Theoretical analysis of the performance of a single side band multicarrier source based on a re-circulating frequency shifter influenced by an optical bandpass filter

Wan Meng (孟 婉)[1], Lixia Xi (席丽霞)[1*], Xiaoguang Zhang (张晓光)[1], Jiachuan Lin (林嘉川)[1], Feng Tian (田 凤)[1], Hao Tu (涂 昊)[1], and Xia Zhang (张 霞)[2]

[1]*State Key Laboratory of Information Photonics and Optical Communications, Beijing University of Posts and Telecommunications, Beijing 100876, China*

[2]*The Key Laboratory of Optical Communications Science and Technology in Shandong Province, Liaocheng University, Liaocheng 252000, China*

[*]*Corresponding author: xilixia@bupt.edu.cn*

Received April 22, 2013; accepted June 28, 2013; posted online August 28, 2013

An optical bandpass filter (OBF) is an important element whose properties considerably influence the output performance of a single side band multicarrier source based on a re-circulating frequency shifter. The influence of the OBF in the loop on the output spectrum is theoretically analyzed. Numerical simulations and experiments are also carried out. Results show that the steepness and deepness of a nonflat-top filter influence the stability of the spectrum of an output multicarrier. To obtain multicarrier output with tone to noise ratio (TNR) >26 dB and error vector magnitude (EVM) <0.25, the steepness ratio of the filter should be greater than 0.75 and deepness should be larger than 0.99.

OCIS codes: 060.2330, 060.2630, 120.2440.
doi: 10.3788/COL201311.090602.

Multicarrier sources have drawn considerable research attention in recent years because they can generate numerous frequency-locked subcarriers—a feature that facilitates Tb/s high-speed optical communication. Tb/s communication systems with multicarrier sources have been experimentally demonstrated; examples of such systems include coherent dense wavelength division multiplexing[1,2] and coherent optical orthogonal frequency division multiplexing[3−5] systems combined with polarization division multiplexed and diverse modulation formats. Multicarrier sources can be constructed by using multiwavelength Er-doped fiber laser[6], cascaded phase and intensity modulators[7], or single side band (SSB) modulators with re-circulating frequency shifters[8−13]. The last technology presents flexible control and accurate frequency spacing at low drive voltage.

In our previous work[14−17], we discussed the influence of the unbalanced factors of an in-phase/quadrature (I/Q) modulator on the performance of a multicarrier source. In this letter, we investigate the effect of an optical bandpass filter (OBF) on multicarrier generation. The OBF in a loop is used to control the output frequency range. The deepness of the OBF attenuates the powers of filtered signals, degrading the output spectrum to tone to noise ratio (TNR). In addition, a carrier's output power varies with carrier frequency because of OBF steepness, resulting in the deterioration of output flatness. These features point to a crucial need to investigate the relationship between OBF properties and output performance.

We theoretically analyze the influence of optical BPF properties on a multicarrier source. Numerical simulation is carried out using filters with different features, including steepness and deepness. The experimental results are in good agreement with the theoretical and numerical simulation results.

The schematic of the multicarrier generator based on recirculation frequency shifer (RFS) is shown in Fig. 1. The configuration is composed of a closed optical fiber loop that comprises a 50:50 optical coupler, an I/Q modulator for frequency shifting, a tunable bandpass filter (BPF) with appropriate bandwidth to control subcarrier number, an Er-doped fiber amplifier (EDFA) to compensate for loop loss, and a PC to control the stabilization of state polarization. The EDFA is located behind the OBF to intensively amplify multicarrier power and reduce noise components falling and beating into the needed subcarrier bandwidth. The amplification improves compensation efficiency.

Assuming that the input optical signal from a continuous-wave (CW) laser is $E_0(t) = A\exp(\mathrm{j}2\pi f_0 t)$, and express the transfer function of the I/Q modulator (which disregards fifth-order crosstalk) as[9]

$$T = \exp(\mathrm{j}2\pi f_m t) + b_3 \exp(-\mathrm{j}6\pi f_m t), \tag{1}$$

where $b_3 = -J_3(\delta_m)/J_1(\delta_m)$ stands for the third-order crosstalk coefficient, $\delta_m = (\pi V_{\mathrm{pp}})/2V_\pi$ denotes the phase modulation depth, and f_m is the frequency shift. The output electronic field after I/Q modulation can be expressed as

$$\begin{aligned} E_1(t) = E_0(t)\cdot T = E_0(t)\cdot \{&\exp(\mathrm{j}2\pi f_m t) \\ &+ b_3\exp(-\mathrm{j}6\pi f_m t)\}. \end{aligned} \tag{2}$$

The influence of the optical filter in the RFS on the spectrum of the multicarrier source are confirmed through analysis in the frequency domain. Thus, the optical signal frequency passed through the OBF in the frequency domain is

$$\begin{aligned} FE_1(f) = {} & A\cdot FE(f - f_0 - f_m)\cdot \mathrm{Filter}(f_0 + f_m) \\ & + Ab_3\cdot FE(f - f_0 + 3f_m)\cdot \mathrm{Filter}(f_0 - 3f_m), \end{aligned} \tag{3}$$

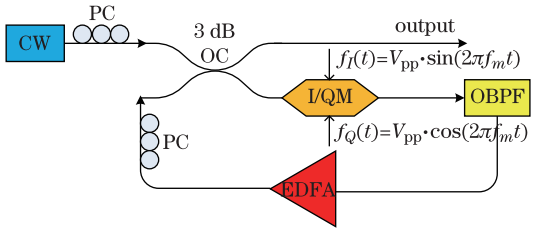

Fig. 1. Diagram of the multicarrier generator based on RFS.

where $FE(f-f_m)$ is the Fourier transformation of Dirac Delta functionexp(j2$\pi f_m t$), f_0+nf_m is denoted as f_n, and Filter(f) stands for the frequency response of the optical filter. Suppose that loss can be precisely compensated by the amplifier. We can obtain the modulated output after the application of an OBF for the first round trip by inverse Fourier transformation from the frequency domain to the time domain

$$E_1(t)=E_0(t)\cdot[1+F(1)T]. \tag{4}$$

$F(n)$ is relevant to Filter(f_n), which changes with filter properties. The frequency-shifted optical signals then recirculate back into the loop through the optical coupler (OC) for the second round trip. The re-modulated signals are affected by the filter terms in the frequency domain. Following the same procedure, we obtain the output after the second round trip thus

$$E_2(t)=E_0(t)\cdot[1+F(1)T+F(1)F(2)T^2]. \tag{5}$$

Therefore, the output traveling the N^{th} round trip can be described as

$$\begin{aligned}E_N(t)=E_0(t)\cdot[1+F(1)\cdot T+F(1)\cdot F(2)\cdot T^2+\\ \cdots+F(1)\cdot F(2)\cdot\cdots\cdot F(N)\cdot T^N].\end{aligned} \tag{6}$$

For an ideal rectangular filter, the frequency response of the optical filter is normalized to

$$\text{Filter}_{\text{R}}(f)=\begin{cases}1 & f_0\leqslant f\leqslant f_n\\ 0 & f=\text{others}\end{cases}. \tag{7}$$

The optical filter in the RFS blocks frequency components higher than f_n, which has the same influence on frequency components ($f_0\sim f_n$). The normalized outputs after the n^{th} round trip in the RFS loop ($n=1,2,\cdots N$) are

$$\begin{aligned}&E_1(t)=E_0(t)\cdot(1+T),\\ &E_2(t)=E_0(t)\cdot(1+T+T^2),\\ &\cdots\\ &E_N(t)=E_0(t)\cdot(1+T+T^2+\cdots+T^N).\end{aligned} \tag{8}$$

In our previous work[9], the output reaches a steady states after (N+4) round trips. However, an actual filter has the shape of nonflat top with roll-off edges at both sides. We analyze the influence of the nonflat-top filter on output signals.

In system simulations, BPFs are often modeled as Gaussian filters, providing a first-step approximation of a real filter[18]. The transfer function of a Gaussian OBF is given by[19]

$$\text{Filter}_{\text{G}}(f)=e^{-\frac{\ln\sqrt{2}\cdot 2^{2k}}{f_{3\,\text{dB}}^{2k}}\cdot(f-f_c)^{2k}}, \tag{9}$$

where f_c represents the central frequency, $f_{3\,\text{dB}}$ denotes a bandwidth of 3 dB, and k is the order of the Gaussian filter. The frequency responses of the Gaussian filter at different (k=1, 2$\cdots$9) filter orders is depicted in Fig. 2(a).

Stop-band attenuation A_{s} is defined as the minimum guaranteed attenuation within the filter stop band, which represents filter deepness. The widely accepted stop-band attenuation $A_{\text{s-accepted}}$ is 40 dB[19], under which the required frequency components are available without power suppression. We define the normalized deepness ratio as $\eta=\frac{A_{\text{s}}}{A_{\text{s-accepted}}}$. The insertion loss (IL) based on the deepness ratio without consideration for constant $IL_{\text{intrinsic}}$ can be described as $IL=A_{\text{s-accepted}}-A_{\text{s}}$, which is closely related to η.

Stop-bandwidth f_{s} is defined as the frequency range of the filter stop band. The difference between the stop-bandwidth and a 3-dB bandwidth affects the steepness of the transfer function[19]. We define the steepness ratio of the transfer function of the filter as $\gamma=f_{3\,\text{dB}}/f_{\text{s}}$, where γ as a function of Gaussian filter order k is presented in Fig. 2(b). Steepness increases with increasing filter order.

Figure 2(a) shows that the frequency response of the first-order Gaussian filter in the 3-dB bandwidth area is nonflat; in the filtering process, this response differentially affects frequency components ($f_0\sim f_n$). The normalized outputs generated after the n^{th} round trip in the RFS loop (n=1, 2, $\cdots$ N) under the first-order filter are

$$\begin{aligned}&E_1(t)=E_0(t)\cdot[1+F(1)T],\\ &E_2(t)=E_0(t)\cdot[1+F(1)T+F(1)F(2)T^2],\\ &\cdots\\ &E_N(t)=E_0(t)\cdot[1+F(1)T+F(1)F(2)T^2+\\ &\qquad\cdots+F(1)F(2)\cdots F(N)T^N].\end{aligned} \tag{10}$$

If $F(n)$ takes the rectangular shape of Eq. (7), Eq. (10) is degraded into Eq. (8). However, a real filter is nonflat-top shaped (e.g., Gaussian-shaped filter), generating a multicarrier output spectrum that differs from that of a rectangular-shaped filter. In contrast to the product of Eq. (8), the output does not reach a steady state because the power stack in each subcarrier differs after N cycles.

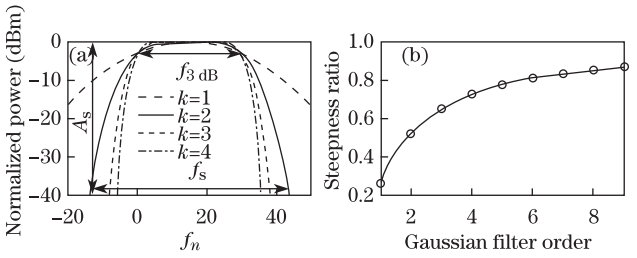

Fig. 2. (a) Gaussian filter frequency responses at different (k=1, 2, 3, 4) filter orders, (b) steepness ratio as a function of the Gaussian filter order.

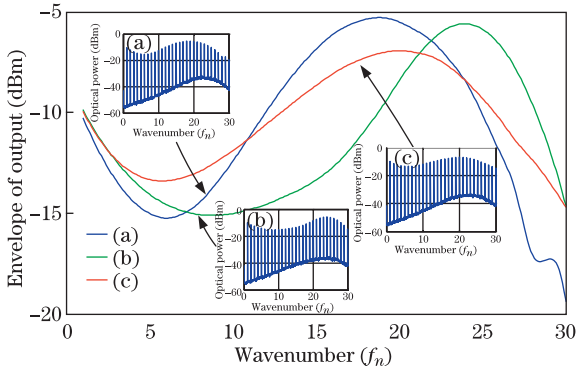

Fig. 3. (color online) Envelope of output spectrum after different re-circulation loops: output spectrum after (a) 70, (b) 78, and (c) 86 circulation loops.

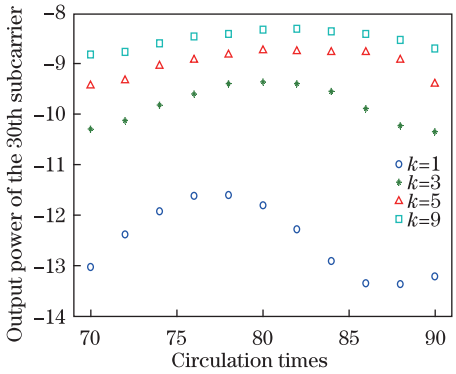

Fig. 4. Optical power of the 30th subcarrier under different Gaussian filter orders at different circulation times.

In the simulation, the power of the CW laser is 12 dBm, the carrier frequency interval is f_m=12.5 GHz, and the modulation depth is $\delta = 0.29$. Assuming that the 3-dB bandwidth of the filter covers the range $f_0 \sim f_0 + 30f_m$, at which 31 carriers are allowed to pass through. The saturated output power of the EDFA is 23 dBm.

We first simulate the output spectrum of the multicarrier generation system under an OBF steepness ratio of 0.27. The envelopes of the output spectrum after different re-circulation loops are displayed in Fig. 3. Insets (a), (b), and (c) show the multicarrier outputs after 70, 78, and 86 rounds of circulation, respectively. The spectra differ for various circulation rounds. That is, the performance of the multicarrier source is unstable because of the nonflat-top filter. The optical power of the 30$^{\text{th}}$ subcarrier under the Gaussian filter of diverse orders after different circulation rounds is also shown in Fig. 4. The results indicate that the stability of the output spectrum could be improved by increasing filter order.

We use the quantity error vector magnitude (EVM) to express the flatness of the output spectrum[20]. It is defined as

$$\mathrm{EVM_{RMS}} = \sqrt{\frac{\frac{1}{N}\sum_{i=1}^{N}|P_i - P_{\mathrm{avg}}|}{P_{\mathrm{avg}}}} * 100\%, \qquad (11)$$

where P_i is the power of the i^{th} subcarrier and P_{avg} is the average power of the output subcarriers. The value of $\mathrm{EVM_{RMS}}$ indicates output spectrum fluctuation. The relationship between steepness ratio γ and $\mathrm{EVM_{RMS}}$, as well as the output spectrum at steepness ratios of 0.27 and 0.87, is illustrated in Fig. 5.

The generated tone spectrum becomes flatter as steepness ratio increases. Figures 5(a) and 5(b) show that a high-quality output spectrum is achieved at a steepness ratio higher than 0.75. In practice, OBFs with high steepness ratios should be selected.

The relationship between the normalized BPF deepness ratio and $\mathrm{EVM_{RMS}}$ is depicted in Fig. 6. The flatness of the generated tone spectrum improves with increasing deepness ratio. Figures 6(a) and 6(b) show the output

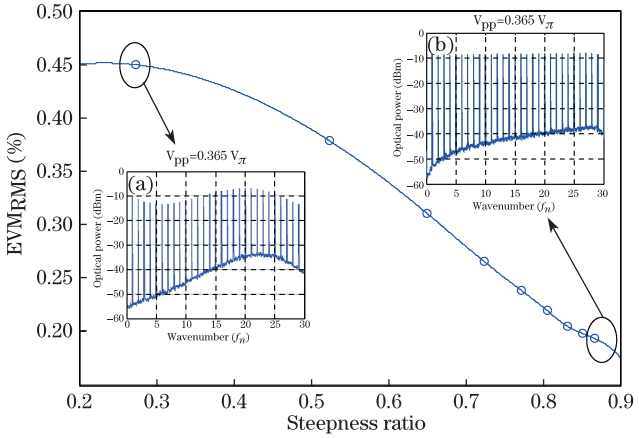

Fig. 5. $\mathrm{EVM_{RMS}}$ as a function of steepness ratio, (a) output spectrum at $\gamma = 0.27$, (b) output spectrum at $\gamma = 0.87$.

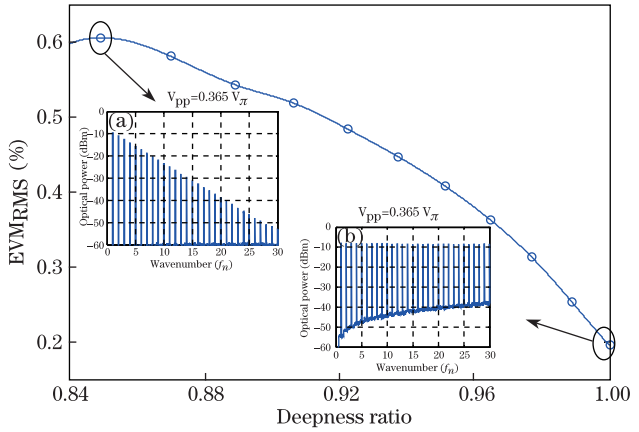

Fig. 6. $\mathrm{EVM_{RMS}}$ as a function of deepness ratio η, (a) output spectrum at $\eta = 0.85$, (b) output spectrum at $\eta = 1$.

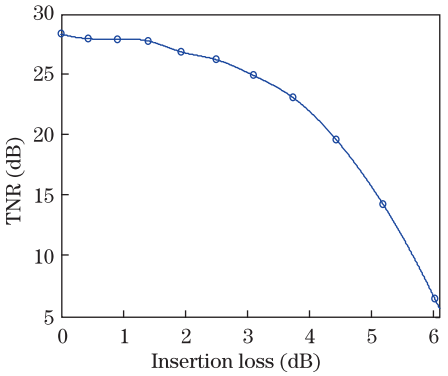

Fig. 7. TNR of the last tone as a function of the insertion loss of OBF.

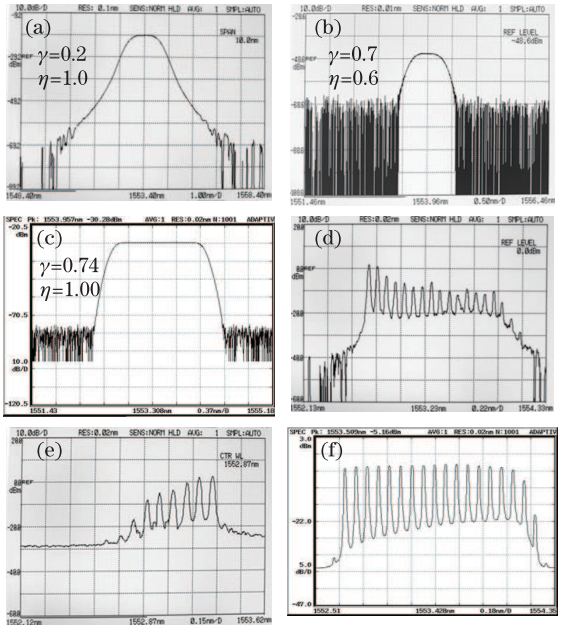

Fig. 8. Output spectra at different filter properties.

spectra at deepness ratios of 0.85 and 1, respectively. Suppressing the power of necessary frequency components can be avoided by appropriately adjusting filter deepness. The relationship between insertion loss (without consideration for constant $IL_{\text{intrinsic}}$) and TNR is displayed in Fig. 7. The TNR of the last subcarrier worsens with increasing IL. The comparison of Figs. 5 and 6 leads us to conclude that the deepness ratio is more important than the steepness ratio. The steepness ratio and deepness should be larger than 0.75 and 0.99, respectively, when an EVM $\leqslant$0.25 is used as the acceptable flatness of multicarriers.

We conduct an experiment (Fig. 1) to further study the effect of OBFs on multicarrier output. The TLS wavelength is run at λ_0=1 553.41 nm, the 3-dB OBF bandwidth is set to 1.4 nm, and the frequency of the RF signal is 10.7 GHz. The saturated output power of EDFA is set to 23 dBm, and the insertion losses of IQM, filter, and OC are approximately 13, 5, and 3 dB, respectively. The experimental results for the OBF with different steepness and deepness states are shown in Fig. 8.

Figures 8(a), 8(b), and 8(c) show the frequency responses of the following filters: Newport TBF-1550-1.0, Lightwave Microsystems AWG 4, and Santec OTF-950, respectively. The output spectrum shown in Fig. 8(d) is unstable and characterized by fluctuations; it corresponds to the filter with a steepness ratio of 0.2 and a deepness ratio of 1. Figure 8(e) shows worse results than those indicated in Fig. 8(d), and the output spectrum in the former corresponds to the filter with a steepness ratio of 0.7 and a deepness ratio of 0.6. A high-quality experimental result is shown in Fig. 8(f), which shows a filter whose steepness ratio is 0.74 and deepness ratio is 1. The experimental results are in good accordance with the theoretical analysis and numerical simulation.

In conclusion, the relationship between the deepness ratio of OBF and the TNR of output spectrum is theoretically analyzed and experimentally demonstrated. The relationship between steepness ratio and output flatness is also investigated. The experimental results accord with the theoretical and numerical analyses. The performance of the output spectrum can be improved by increasing filter steepness ratio and deepness ratio. The OBF in the RFS loop has an important function in obtaining high-quality and stable multicarriers.

This work was supported by the National Natural Science Foundation of China (No. 61205065), Specialized Research Fund for the Doctoral Program of Higher Education of China (No. 20110005110014), and Provincial Natural Foundation of Shandong (No. ZR2010FM043).

References

1. H. Suzuki, M. Fujiwara, and K. Iwatsuki. J. Lightwave Technol. **24,** 1998 (2006).
2. G. Gavioli, E. Torrengo, G. Bosco. A. Carena, V. Curri, V. Miot, P. Poggiolini, M. Belmonte, F. Forghieri, C. Muzio, S. Piciaccia, A. Brinciotti, A. La Porta , C. Lezzi, S. Savory, and S. Abrate, in *Proceedings of Conference on Optical Fiber Communications* OThD3 (2010).
3. Q. Yang, Z. He, and W. Liu, in *proceedings of Conference on Optical Fiber Communications* JThA35 (2011).
4. X. Liu, S. Chandrasekhar, and X. Chen, in *european conference and exhibition on optical communications* Th.13B (2011).
5. J. Yu, Z. Dong, J. Zhang, X. Xiao, H.-C. Chien, and N. Chi, J. Lightwave Technol. **30,** 458 (2012).
6. M. A. Mirza and G. Stewart, J. Lightwave Technol. **27,** 1034 (2009).
7. S. Zou, Y. Wang, Y. Shao, J. Zhang, J. Yu, and N. Chi, Chin. Opt. Lett, **10,** 070605 (2012).
8. X. Liu, S. Chandrasekhar, B. Zhu, and D. W. Peckham, in *proceedings of Conference on Optical Fiber Communications* OWO2 (2009).
9. J. Li, X. Li, and X. Zhang. Opt. Express **18,** 19876 (2010).
10. F. Tian and X. Zhang, J. Lightwave Technol. **29,** 8 (2011).
11. J. Zhang, J. Yu, N. Chi, Z. Dong, X. Li, Y. Shao, and L. Tao, Opt. Lett. **37,** 4050 (2012).
12. X. Li, J. Yu, Z. Dong, J. Zhang, Y. Shao, and N. Chi, Opt. Express **20,** 21833 (2012).
13. J. Zhang, J. Yu, N. Chi, Y. Shao, L. Tao, Y. Wang, and X. Li, IEEE Photon. Technol. Lett. **24,** 16 (2012).
14. J. Li, X. Li, X. Zhang, F. Tian, and L. Xi, in *Proceedings of European Conference and Exhibition on Optical Communications* P3.05 (2010).
15. J. Li, X. Li, X. Zhang, F. Tian, and L. Xi, Opt. Express **18,** 17597 (2010).
16. H. Zhou, L. Xi, J. Li, X. Zhang, and N. Liu, Chin. Opt. Lett. **10,** 100602 (2012).
17. L. Xi, J. Li, X. Zhang, F. Tian, and W. Zhang, Chin. Phys. B **20,** 084202 (2011).
18. M. Seimetz, *High-Order Modulation for Optical Fiber Transmission* (Springer, Atlana, 2009).
19. VPIsystems, Photonic Modules Reference Manual, (2005).
20. R. A. Shafik, S. Rahman, and R. Islam, in *Proceedings of the International Conference on Electrical and Computer Engineering* 408 (2006).